PHYSICAL REVIEW B VOLUME 47, NUMBER 3 15 JANUARY 1993-I

Quantum confinement in semiconductor heterostructure nanometer-size particles

Joseph W. Haus*
Research Center for Advanced Science and Technology, University of Tokyo, 4-6-1 Komaba, Meguro-ku, Tokyo 153, Japan

H. S. Zhou, I. Honma, and H. Komiyama
Department of Chemical Engineering, Faculty of Engineering, The University of Tokyo, Bunkyo-ku, Tokyo 113, Japan
(Received 23 June 1992; revised manuscript received 24 August 1992)

Nanometer-size semiconductor particles coated with another semiconductor can exhibit unusual and interesting phenomena associated with the redistribution of the electron and hole wave functions. Using the band offsets and effective masses, the overlap of the electron and hole wave functions can be altered by changing the core radius of the particles. The theory can incorporate multiple shells, band bending, and charge effects. An efficient method for solving the equations is given.

I. INTRODUCTION

Quantum confinement of carriers in semiconductors has been accomplished by methods as disparate as epitaxial growth, etching, sputtering, and precipitation chemistry. Precise control over optical or electrical properties is the desired goal of these research directions. The quantum properties of carriers in nanometer-size particles has received wide attention because it provides a study, albeit with limitations on control of the size and defects, of carrier confinement in three dimensions.

Quantum-confinement effects on the absorption for direct-band-gap materials was reported early,[1] but it was later detailed experiments that established the field.[2] The semiconductor types were at first the II-VI semiconductors[3,4] or I-VII compounds,[2] most have Γ-point direct band gaps, but CdTe with an L-point gap has also been examined.[5] Recently III-V semiconductor particles have also been synthesized.[6]

The indirect-band-gap materials, Si nanostructures[7] and Ge nanometer-size particles,[8] have also created considerable discussion in the scientific community because of their efficient luminescence in the visible regime. Experiments on particles, both direct and indirect band gaps, are attempting to elucidate fundamentally important processes that describe the observed phenomena and possibly set directions for future technology.[9]

Coated particles offer a challenge to synthesis, but they also provide insights in the quantum confinement of carriers. Interest in these materials is partially motivated by the development of optical properties that mimic the superior performance characteristics of atoms or molecules. Control over the coating thickness gives a further engineering degree of freedom to elucidate the underlying physics of these structures; by changing the thickness of the shell and the particle radius, the overlap of the wave functions and the band gap can be changed. This is distinct from the change in the wave-function overlap caused by the finite height of the host material;[10] in coated particles, the outer material can be chosen to have a smaller band gap, thus favoring the shift of the wave-function maximum from the particle center toward the outer boundary.

In coated particles, we will show here, for example, that the carriers can spatially separate in the materials due to the band offset and mass differences among the carriers. We will henceforth call these particles "heterostructures" because they have two different materials, in this case semiconductors, with an interface between them. The physical parameters of each semiconductor material will have a great influence on the optical properties, such as the luminescence, of the heterostructure particle. In fact, type-II-like heterostructures can be achieved in the coated particles, where the electrons and holes are spatially separated. Charging and band-bending effects can also be studied and modeled within the context of the coated particles; these effects may also be treated by the method developed here.

In this paper we will develop a theoretical treatment of heterostructure semiconductor particles based on the single band effective-mass approximation. It offers a simple analytical method to investigate the quantum confinement of the carriers. However, such models have limitations and we will return to this in the results section, where delimitations of the approximations will be examined. Several types of direct-band-gap materials will be selected for numerical computations and our discussion will be based on those results; two of the systems have been synthesized in the laboratory, they are the ZnS/CdSe (Ref. 11) and CdS/PbS (Ref. 12) particles; here our notation denotes the (core-shell) materials. The third heterostructure particle is the InP/InAs system, which has been well studied as quantum-well structures and for which parameters, such as the electron and the hole masses and the band offsets, are available. These materials are used to illustrate some of the interesting phenomena that can occur. Coulomb effects between the electron and hole, and incomplete confinement of the carriers can also be significant.[10] In the strong confinement regime, where the particle is smaller than the bulk exciton radius, the dominant contribution to the carrier's energy is the kinetic energy imposed by the boundary conditions.

We note that the confinement of the carriers to the particle is not a necessary assumption, but is adopted for convenience. For instance, when homogeneous CdS particles are embedded in an insulating medium with a band gap of 7 eV, the energy is lowered by about 0.2 eV for the smallest particle radius (2 nm) considered in this paper.[10] We generally take a smaller band-gap material for the shell layer, so the confinement in heterogeneous particles will be stronger.

The Coulomb interaction can be treated with the help of the wave functions developed from the strong confinement regime. There will, depending on the specific materials and particle dimension, be significant contributions from this energy.[13] This could lead to interesting quantum effects for the quantum dots, but that is beyond the scope of this paper. Here we want to establish effects that are based on the quantum confinement. We study the electron and hole wave functions, the shift of the band-gap energy, and the overlap of the wave functions.

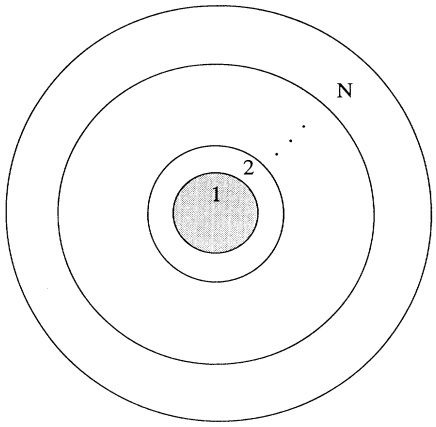

FIG. 1. A diagram of a spherical particle with N regions. The wave function does not penetrate the region beyond the outer boundary of the Nth shell.

II. ANALYSIS

The theoretical analysis starts with the effective-mass approximation with single bands for both the conduction- and valence-band carriers. The single carrier envelope wave functions are used in each band. We restrict our analysis to the strong confinement regime where the Coulomb interaction between particles can be neglected in comparison with the confinement energies. The Schrödinger equation for the envelope function in each band, labeled by the subscript $\alpha=e$ (electron) or h (holes), is

$$\left[-\frac{h^2}{2}\nabla\cdot\frac{1}{m_\alpha}\nabla+V_\alpha(\mathbf{r})\right]\psi_\alpha=E_\alpha\psi_\alpha\ . \tag{1}$$

The mass m_α may depend on the position in the heterostructure particle. The particle may contain several layers (see Fig. 1), each with different potential values and different masses for the carriers. This form of the Schrödinger equation conserves the probability when the mass is variable. For spherical particles with spherically symmetric coatings and homogeneous potentials and masses, the analytical solution of Eq. (1) for the nth region, as shown in Fig. 1, can be written as

$$\psi_{lm}^{\alpha n}=[A_{lm}^{\alpha n}j_l(k_{\alpha n}r)+B_{lm}^{\alpha n}n_l(k_{\alpha n}r)]Y_{lm}(\theta,\phi)\ , \tag{2}$$

where

$$k_{\alpha n}=\left[\frac{2m_{\alpha n}(E_\alpha-V_{\alpha n})}{h^2}\right]^{1/2}\ ; \tag{3}$$

$j_l(z)$ and $n_l(z)$ are the spherical Bessel and Neumann functions and $Y_{lm}(\theta,\phi)$ are the spherical harmonics.[14] The potential and mass of the carrier in the nth region have been labeled with a subscript αn. We will assume that there are N regions altogether, so the index n has a range from 1 to N; the radius of the Nth could extend to infinity and the effect of incomplete confinement included in the analysis;[10] we do not do that here for simplicity, since it would add further parameters. We simply assume that the insulator band gap is large enough to confine the carriers. The energy parameters for the valence and conduction band of a heterostructure particle with a single shell are shown in Fig. 2. The potential in the core is used as the zero reference energy in this paper.

At each shell boundary r_n, the continuity of the wave function and the probability current give the following relations between the unknown amplitudes $\{A_{lm}^{\alpha n},B_{lm}^{\alpha n}\}$:

$$A_{lm}^{\alpha n}j_l(k_{\alpha n}r_n)+B_{lm}^{\alpha n}n_l(k_{\alpha n}r_n)=A_{lm}^{\alpha n+1}j_l(k_{\alpha n+1}r_n)+B_{lm}^{\alpha n+1}n_l(k_{\alpha n+1}r_n)\ ; \tag{4}$$

$$\frac{k_{\alpha n}}{m_{\alpha n}}[A_{lm}^{\alpha n}j_l'(k_{\alpha n}r_n)+B_{lm}^{\alpha n}n_l'(k_{\alpha n}r_n)]=\frac{k_{\alpha n+1}}{m_{\alpha n+1}}[A_{lm}^{\alpha n+1}j_l'(k_{\alpha n+1}r_n)+B_{lm}^{\alpha n+1}n_l'(k_{\alpha n+1}r_n)]\ .$$

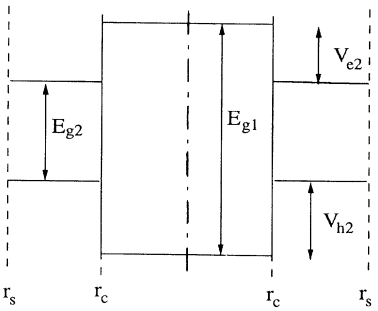

FIG. 2. Schematic view of the potential energies for the electron and hole. The band gaps E_{gn} and valence-band offsets V_{hn} are displayed for each material; $n=1$ (core) and $n=2$ (shell).

The prime on the spherical Bessel functions denotes a derivative with respect to the argument. At the outer shell boundary, we assume that the wave function $\psi_{lm}^{\alpha N}$ vanishes. For each spherical harmonic amplitude the relation at the outer boundary is

$$A_{lm}^{\alpha N} j_l(k_{\alpha N} r_N) + B_{lm}^{\alpha N} n_l(k_{\alpha N} r_N) = 0 \ . \tag{5}$$

The coefficients of the outer shell wave function $A_{lm}^{\alpha N}$ and $B_{lm}^{\alpha N}$ are related to the coefficient of the center $A_{lm}^{\alpha 1}$ through application of a recursion formula generated from the boundary conditions, Eq. (4). The general result for the recursion formula, after use of the Wronskian for the spherical Bessel functions, is defined as

$$W(z) = j_l(z) n_l'(z) - j_l'(z) n_l(z) \ , \tag{6}$$

and the definition $\eta_{\alpha n} = k_{\alpha n}/m_{\alpha n}$ is

$$A_{lm}^{\alpha n+1} = -\frac{(k_{\alpha n+1} r_n)^2}{\eta_{\alpha n+1}} [\{ \eta_{\alpha n+1} n_l'(k_{\alpha n+1} r_n) j_l(k_{\alpha n} r_n) - \eta_{\alpha n} n_l(k_{\alpha n+1} r_n) j_l'(k_{\alpha n} r_n) \} A_{lm}^{\alpha n} + \{ \eta_{\alpha n+1} n_l'(k_{\alpha n+1} r_n) n_l(k_{\alpha n} r_n) - \eta_{\alpha n} n_l(k_{\alpha n+1} r_n) n_l'(k_{\alpha n} r_n) \} B_{lm}^{\alpha n}] \ , \tag{7a}$$

$$B_{lm}^{\alpha n+1} = -\frac{(k_{\alpha n+1} r_n)^2}{\eta_{\alpha n+1}} [\{ \eta_{\alpha n+1} j_l'(k_{\alpha n+1} r_n) j_l(k_{\alpha n} r_n) - \eta_{\alpha n} j_l(k_{\alpha n+1} r_n) j_l'(k_{\alpha n} r_n) \} A_{lm}^{\alpha n} + \{ \eta_{\alpha n+1} j_l'(k_{\alpha n+1} r_n) n_l(k_{\alpha n} r_n) - \eta_{\alpha n} j_l(k_{\alpha n+1} r_n) n_l'(k_{\alpha n} r_n) \} B_{lm}^{\alpha n}] \ . \tag{7b}$$

This recursion method can be easily numerically implemented to determine the general energy eigenvalues of a heterostructure particle. Radial inhomogeneities in the effective masses and the potential can be explored by this method. For the special case $N=2$ of a core and shell (refer to Fig. 2; r_c, r_s are the radii in the core and shell region, respectively), the shell coefficients generated from Eqs. (7) are

$$A_{lm}^{\alpha s} = -\frac{(k_{\alpha 2} r_c)^2}{\eta_{\alpha 2}} \{ \eta_{\alpha 2} n_l'(k_{\alpha 2} r_c) j_l(k_{\alpha 1} r_c) - \eta_{\alpha 1} n_l(k_{\alpha 2} r_c) j_l'(k_{\alpha 1} r_c) \} A_{lm}^{\alpha c} \tag{8a}$$

and

$$B_{lm}^{\alpha s} = -\frac{(k_{\alpha 2} r_c)^2}{\eta_{\alpha 2}} \{ \eta_{\alpha 2} j_l'(k_{\alpha 2} r_c) j_l(k_{\alpha 1} r_c) - \eta_{\alpha 1} j_l(k_{\alpha 2} r_c) j_l'(k_{\alpha 1} r_c) \} A_{lm}^{\alpha c} \ . \tag{8b}$$

The energy levels are obtained by substituting these expressions into $\psi_{lm}^{\alpha s}(r_s)$, Eq. (5), and changing the energy E_α to obtain the zeros in Eq. (5).

The overlap integrals for a p-type valence band and an s-type conduction band, relating the ability of the electron and hole carriers to directly recombine is given by

$$F_{lm} = \left| \int_0^{r_N} \psi_{lm}^{h*}(r) \psi_{lm}^{e}(r) r^2 dr \right| \ . \tag{9}$$

Here we assume that the envelope wave functions have been normalized to unity and a direct band gap, where the Bloch functions, not treated here, have the same oscillation wave vector. This method will be used to obtain specific results in the following section.

III. RESULTS

The analysis of the preceding section is used to calculate several important quantities. For simplicity we will only report the shift of the lowest energy state $l=0$. As mentioned above, we will consider the simplest heterostructure particle, one that has a core and only one shell. The influence of band bending and alloying will not be considered. In Table I the material parameters provide the vital information used in evaluating the wave functions and eigenenergies of the carriers.[15–22] The band gaps of each semiconductor and valence-band offset parameter, V_{h2}, relations are displayed in Fig. 2. The parameter V_{e2} is obtained from these data, as in Fig. 2. All our particles will have the large band-gap material in the core and the small band-gap material will be the shell. The table uses the light-hole masses for each material because these will have the greatest influence on the shift of the band-gap energy. Anisotropy of the masses requires a perturbational treatment that is not undertaken here.

The CdS/PbS heterostructure has equal electron and hole masses in the PbS material, so that the differences between the electron and hole masses in the core, as well as the band offset, constitute the only influences on the wave function within this model. The CdS lattice is a wurtzite structure and the PbS lattice has a rocksalt structure. The two-band model for PbS is quite good; other bands are separated by about 2.5 eV from the these bands.[23,24] The anisotropy of the bands is also small so

TABLE I. Material parameters. All energies are in eV and the mass m_0 is the free-electron mass. The references are in square brackets.

Material	m_e/m_0	m_n/m_0	Band gap	Conduction-band offset
CdS [15]	0.2	0.7	2.5	1.2[21]
PbS [16]	0.085	0.085	0.4	
ZnS [17]	0.28	0.49	3.9	0.9[21]
CdSe [18]	0.13	0.45	1.84	
InP [19]	0.079	0.65	1.34	0.4[22]
InAs [20]	0.023	0.42	0.36	

that the isotropic band model is reasonably good; however, as concluded by Wang *et al.*[24] due to electron and hole correlations, the effective-mass approximation overestimates the confinement energy of a homogeneous particle by about a factor of 2 when the radius is 2 nm. The energies are lower than the effective-mass model predicts.

The CdS two-band model also needs some clarification; for the size range we cover here (2–10 nm) the hole energies are shifted by only a small amount due to the large effective masses and the mixing of other bands is small. Cluster band-structure calculations[25–28] support this conclusion over the size range of our results. The Coulomb energy is negligible in PbS owing to the large relative dielectric constant of 18.5; however, in homogeneous CdS calculations including Coulomb energy and incomplete confinement give a correction[10,28] of about -0.25 eV at the smallest radii we investigate; the Coulomb correction is inversely proportional to the radius. The valence-band offset energy was derived from an expression of Nethercot.[21]

Figure 3 is a plot of the total band gap, $E_g = E_{g1} + E_e + E_h$, versus particle shell radius r_s (from 2 to 10 nm) and the ratio of the shell thickness versus the particle outer radius is defined as

$$R = (r_s - r_c)/r_s \ , \tag{10}$$

its range is from 0 to 1. E_{g1} is the band-gap energy of the core material (Fig. 2); the energies E_e and E_h can be negative when the shell material has a smaller band gap, as in this case. The shading in the figure corresponds to the area between two contour lines separated by 0.5 eV. The band gap in the two limiting cases: $R = 0$ and 1 are the quantum-confinement band gaps of the homogeneous semiconductor material. The band gap is not monotonic as the ratio R is changed, an effect which is especially pronounced in the thin shell regime. The mass of the carriers in the PbS shell is so light that the band-gap energy of the PbS particle becomes comparable to that of the CdS particle at $r_s = 2$ nm.

Even though the band gap of the shell material is smaller and the potential for each carrier is lower in the shell, a maximum can appear, because there is a competition between the kinetic energy and the potential energy in these heterostructures. The larger masses of the carriers in the core favor localizing the carrier there to minimize the energy; the masses of the carriers in the shell are

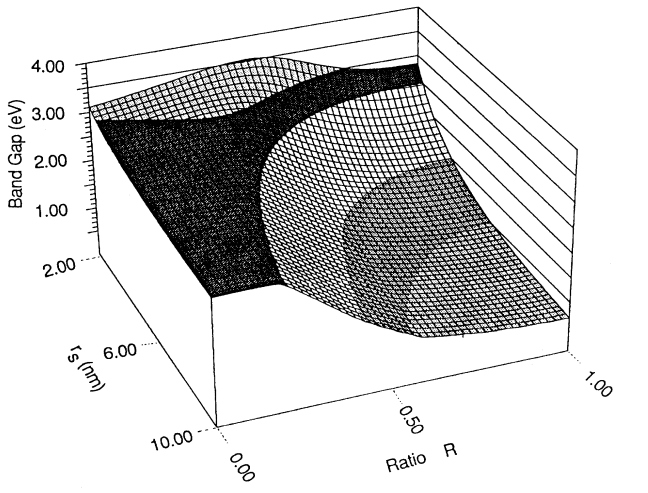

FIG. 3. The band-gap energy of the ground state for the CdS/PbS heterostructure particle vs particle shell radius r_s and the ratio of the shell thickness to the outer radius R, see Eq. (10). The shading in this and later pictures corresponds to the area between two contour lines shown by the lines of the vertical axes.

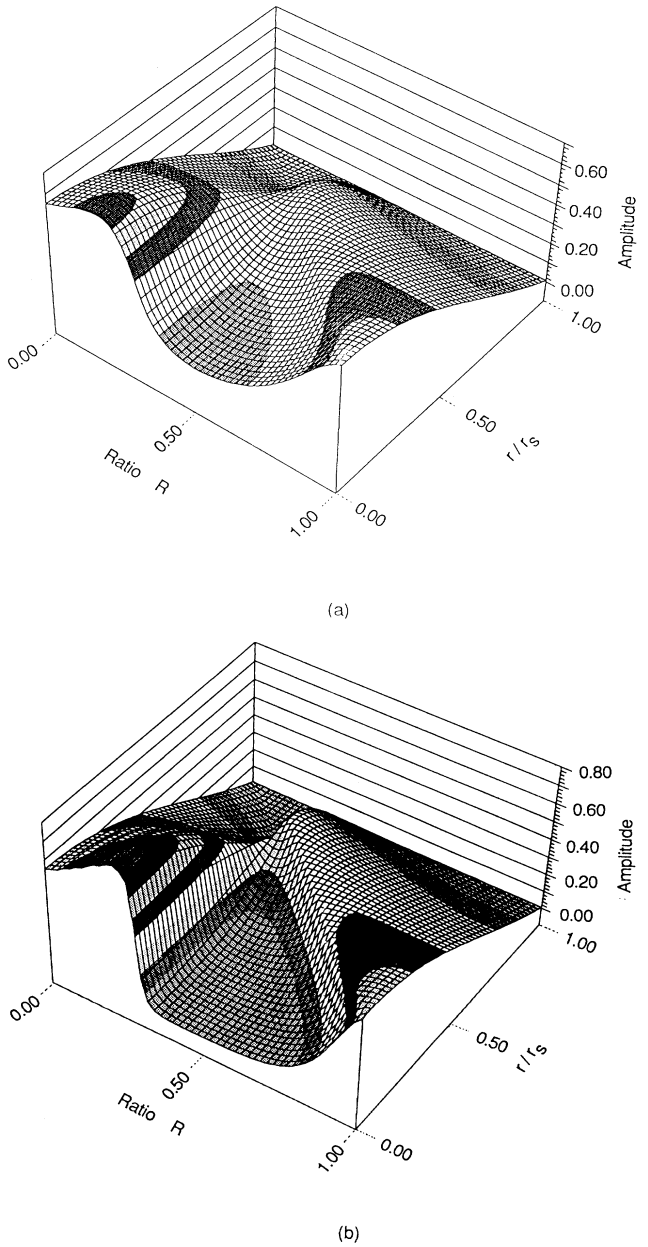

FIG. 4. The (a) electron and (b) hole squared amplitudes for a CdS/PbS particle with shell radius 4 nm. The R dependence is also displayed.

so light that the carriers pay a large penalty in the kinetic energy for extending into the shell. For this case both the electron and the hole wave functions at the center of the particle are increased as the shell is added, while keeping the size of the particle constant. The effect is more pronounced in the hole wave function though, because the hole mass is heavier in the core.

The square amplitudes of the electron and hole wave functions are given in Figs. 4 for a particle that has a shell radius $r_s = 4$ nm. At the two extreme values of R, the wave function has the form of a homogeneous particle. As R is changed, the wave function becomes distorted. For small shell radii, the wave function becomes more concentrated in the center, due to the competition between the kinetic-energy and potential-energy contributions previously mentioned. Eventually though, the potential energy dominates and the carriers shift their wave-function maximum toward the shell boundary. Due to the different band offsets and carrier masses in each case though, the electron and hole wave functions change at different rates.

A good measure of the difference between the two wave functions is the overlap integral of the envelope wave functions, Eq. (9). This is plotted for the CdS/PbS particle in Fig. 5; the particle shell radius is taken as 4 nm and the inset displays the relationship between the band gaps and the band offsets for the core and shell materials. For thin shells the hole wave function, because of its heavier mass in CdS, has a larger increase in the density in the core than does the electron wave function. This causes an initial decrease of the overlap in Fig. 5. However, as the ratio R, defined in Eq. (10), is increased, the larger valence-band offset for the hole shifts the hole wave function toward the shell region. This occurs for $R \approx 0.35$ and the overlap has a minimum at about $F \approx 0.85$. The small peak in the overlap integral around $R \approx 0.25$ occurs because the hole wave function rapidly shifts its weight from the core to the shell in this region and as it does, there is a value where the electron and hole wave functions are close to one another again [see Fig. 4(b)]. Again, a word about the incomplete confinement of the carriers; this will also have an effect on the energies[10] and on the overlap. The band gap of the insulating host is usually around 7 eV and for the small band-gap PbS material it will not significantly change the results. We have chosen a radius in Fig. 5 for which this effect in CdS is less than 0.05 eV.[10]

The ZnS/CdSe heterostructure particles have nearly equal hole masses for the core and shell material. Both are wurtzite lattice structures. The band-gap energy of the core is in the ultraviolet and there is a 2-eV difference between the band gap of the core and shell material. Cluster calculations show that for homogeneous ZnS particles,[25,28] and CdSe particles,[29] the effective-mass approximation holds over the size range considered here. The band offset is larger for the electrons, which would favor shifting their wave-function amplitude toward the shell, but this is again in competition with the electron masses for these materials. The holes have a much heavier mass, hence their kinetic-energy contribution to the band-gap shift is much reduced. Figure 6 shows that the shifts of the band gap for the homogeneous particles are much smaller than before. There is only a slight rise of the band-gap energy at the smallest outer shell radius of 2 nm; this effect was also observed for the effective-mass model in Ref. 3 for these particles.

As for the CdS/PbS particles, the wave functions of the electrons and the holes shift their amplitudes toward the shell. For the ZnS/CdSe particles though, the shift occurs for larger values of R due to the greater dominance of the potential energy. The hole has no competition between the potential and kinetic energies and is able to shift its amplitude toward the shell first. The overlap integral, shown in Fig. 7, exhibits a sharp, deep minimum

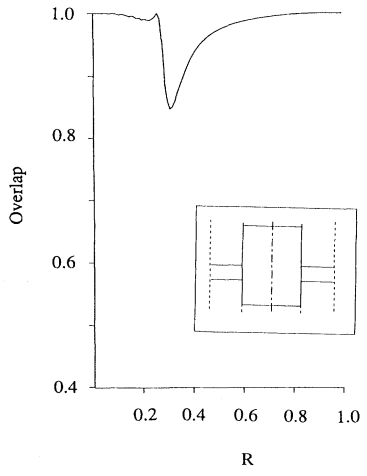

FIG. 5. The overlap integral, as defined in Eq. (9), is plotted vs the ratio R for a CdS/PbS particle with a shell radius of 4 nm. The inset shows the scale of the band gaps and offset for the semiconductors, refer to Fig. 2.

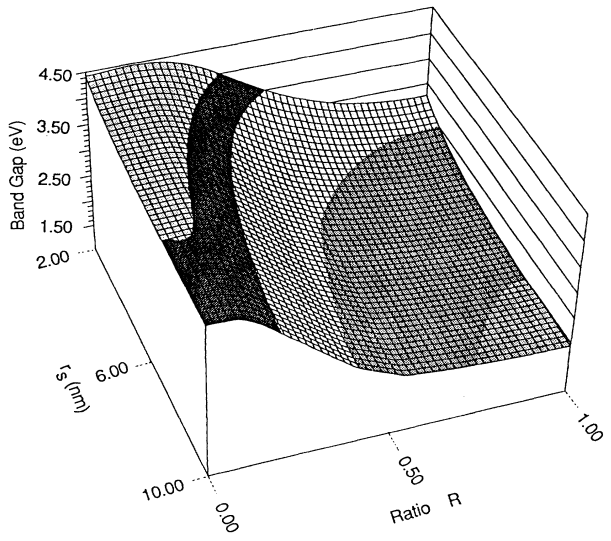

FIG. 6. Band-gap energy for the ZnS/CdSe heterostructure particle vs r_s and R.

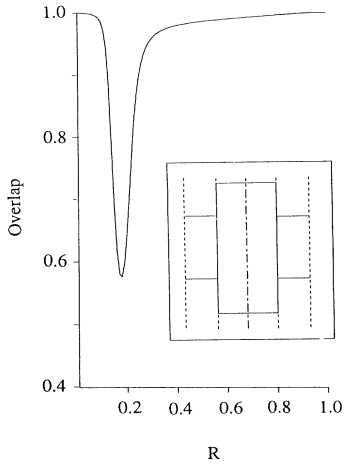

FIG. 7. Overlap integral for a 4-nm radius ZnS/CdSe particle vs R. The inset has the same interpretation as in Figs. 2 and 5.

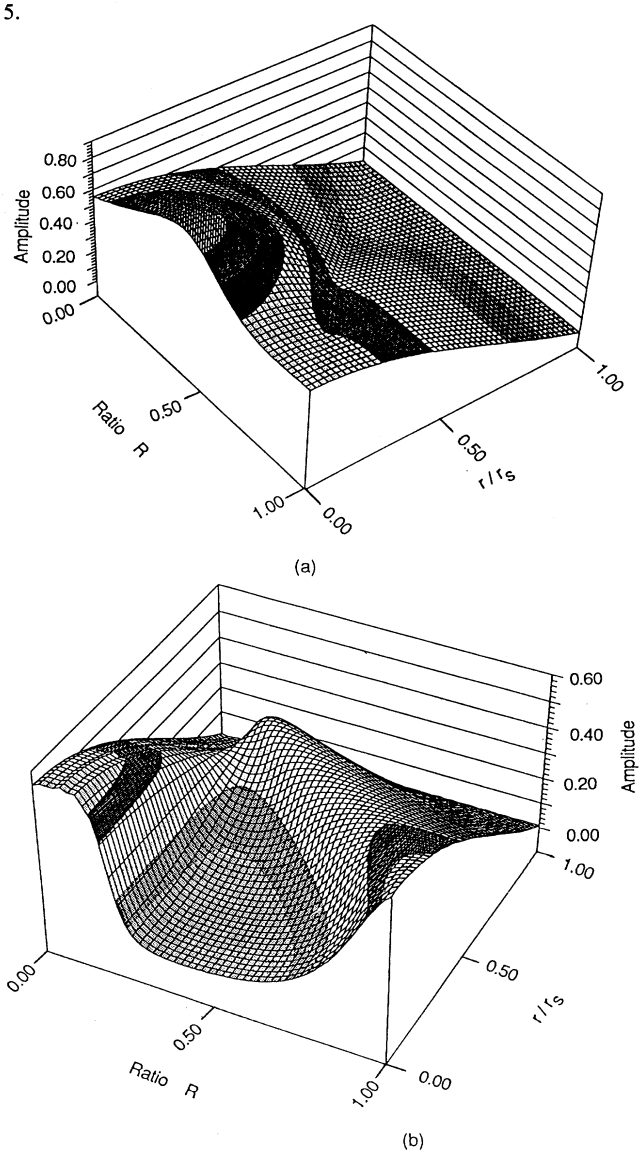

FIG. 8. (a) Electron and (b) hole square amplitude for an InP/InAs particle vs R and r. The particle has a 4-nm radius.

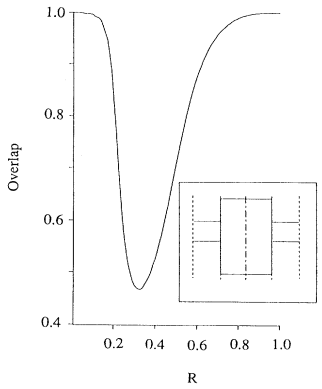

FIG. 9. Overlap integral for the 4-nm radius InP/InAs particle vs R. See Figs. 2 and 5 for the interpretation of the inset.

around $R \approx 0.2$ as the hole wave function shifts followed by the electron wave function.

The InP/InAs particle is interesting because the electron masses in both materials are small; both have a zinc-blende structure. Thus, for sufficiently small particles, their kinetic energy will exceed the depth of the shell potential well; as a consequence there is less tendency for the electron to shift its density toward the shell. The situation of a material that separates the electron and the hole wave functions is displayed in Fig. 8 for a 4-nm radius particle. The amplitude of the electron has a pronounced increase in the core and remains there for all values of the shell thickness ratio.

The hole wave function in Fig. 8(b) has a shift toward the shell material as the potential contribution dominates. The overlap integral of Fig. 9 has a broad deep minimum and a value of less than 0.5; this particle separates the electron and hole wave functions in two regions of the particle. It should show the possibility of engineering semiconductor heterostructure particles with significant separation between the electron and holes.

IV. SUMMARY

We have provided a recursive method to find the wave functions and energies of the carriers in a heterostructure particle. The hole and the electron wave functions are treated with spherically symmetric boundary conditions. It can be used to study band bending and alloying effects by dividing the particle into a number of shells each with a constant potential and constant mass for each carrier. The effects of interaction between the carriers, such as polarization and Coulombic interactions, can be included in a perturbational treatment and they could prove especially interesting for those particles that have a small overlap, as the InP/InAs particles discussed in the preceding section.

The electron and the hole wave functions can be separated in specific materials; an effect which largely depends on the carrier masses. Generally, it will happen in situations that mimic the InP/InAs particle; the electron masses in the shell material should be much lighter than in the core and the particle radius small enough, so that

the shift of the kinetic energy exceeds the potential-well depth in the shell. In this case the electrons are repelled from the surface and toward the center. The holes being heavier undergo the usual shift toward the shell region when the shell becomes thick enough.

We also found a tendency for the wave-function amplitude to increase in the center, when shell material of a smaller band gap is added to the particle, while keeping the radius constant. This is a mass effect that occurs when the carrier mass in the center is heavier than the mass in the shell. For thin shells, the kinetic-energy increase required for the wave function to extend into the shell exceeds the decrease of potential energy for the carriers. The particle is effectively repelled from the shell.

Heterostructure particles may display a variety of interesting results, such as an increase of the absorption band edge when the shell material has a small band gap and rapid changes in the luminescence efficiency. The heterointerface may also be studied here and effects of defects need to be assessed. The material parameters studied here are available for a wide range of materials and the challenge of fabricating particles with specific properties lies ahead.

ACKNOWLEDGMENTS

We thank Professor E. Hanamura and Dr. V. A. Sharkin for interesting and fruitful discussions on this topic.

*Permanent address: Physics Department, Rensselaer Polytechnic Institute, Troy, NY 12180-3590.

[1]C. R. Berry, Phys. Rev. **161**, 848 (1967).
[2]A. I. Ekimov and A. A. Onuschchenko, Fiz. Tekh. Poluprovodn. **16**, 1215 (1982) [Sov. Phys. Semicond. **16**, 775 (1982)].
[3]L. E. Brus, J. Chem. Phys. **79**, 5566 (1983).
[4]N. F. Borrelli, D. W. Hall, H. J. Holland, and D. W. Smith, J. Appl. Phys. **61**, 5399 (1987); S. Hayashi, H. Sanda, M. Agata, and K. Yamamoto, Phys. Rev. B **40**, 5544 (1989).
[5]M. A. Olshavsky, A. N. Goldstein, and A. P. Alivasatos, J. Am. Chem. Soc. **112**, 9438 (1990).
[6]B. G. Potter and J. H. Simmons, Phys. Rev. B **43**, 2234 (1991).
[7]S. Furukawa and T. Miyasato, Jpn. J. Appl. Phys. **27**, L2207 (1988); S. Hayashi, M. Fujii, and K. Yamamoto, *ibid.* **28**, L1464 (1989); H. Takagi, H. Ogawa, Y. Yamazaki, A. Ishizaki, and T. Nagagiri, Appl. Phys. Lett. **56**, 2379 (1990); L. T. Canham, *ibid.* **57**, 1046 (1990).
[8]Y. Maeda, N. Tsukamoto, Y. Yazawa, Y. Kanemitsu, and Y. Masumoto, Appl. Phys. Lett. **59**, 3168 (1991).
[9]Recent reviews: C. Flytzanis, F. Hache, M. C. Klein, D. Ricard, and P. Roussignol, Prog. Opt. **29**, 322 (1991); M. G. Bawendi, M. L. Steigerwald, and L. E. Brus, Ann. Rev. Phys. Chem. **41**, 477 (1990).
[10]Y. Kayanuma and H. Momoji, Phys. Rev. B **41**, 10 261 (1990).
[11]A. R. Kortan, R. Hull, R. L. Opila, M. G. Bawendi, M. L. Steigerwald, R. J. Carroll, and L. E. Brus, J. Am. Chem. Soc. **112**, 1322 (1990).
[12]H. S. Zhou, I. Honma, H. Komiyama, and J. W. Haus (unpublished).
[13]V. A. Sharkin and E. Hanamura (private communication).
[14]See *Handbook of Mathematical Functions*, edited by M. Abramowitz and I. A. Stegun (Dover, New York, 1972); they use $y_1(z)$ instead of $n_1(z)$ for the Neumann functions.
[15]D. G. Thomas and J. J. Hopfield, Phys. Rev. **116**, 573 (1959); J. J. Hopfield and D. G. Thomas, *ibid.* **122**, 35 (1961).
[16]R. Dalven, in *Solid State Physics*, edited by H. Ehrenreich, F. Seitz, and D. Turnbull (Academic, New York, 1973), Vol. 28, pp. 200 and 209.
[17]J. C. Miklosz and R. G. Wheeler, Phys. Rev. **153**, 913 (1967).
[18]J. O. Dimmock and R. G. Wheeler, J. Appl. Phys. **32**, 2271 (1962); R. G. Wheeler and J. O. Dimmock, Phys. Rev. **125**, 1805 (1962).
[19]L. W. James, J. P. van Dyke, F. Herman, and D. M. Chang, Phys. Rev. B **1**, 3998 (1970); P. Rochon and E. Fortin, *ibid.* **12**, 5803 (1975); Q. H. F. Vrehen, J. Phys. Chem. Solids **29**, 129 (1968).
[20]F. Lukes, Phys. Status Solidi B **84**, K113 (1977); C. W. Litton, R. B. Dennis, and S. D. Smith, J. Phys. Chem. Ser. **2**, 2146 (1969); F. Matossi and F. Stern, Phys. Rev. **111**, 472 (1958).
[21]A. N. Nethercot, Phys. Rev. Lett. **33**, 1088 (1974).
[22]J. A. van Vechten, Phys. Rev. **187**, 1007 (1969).
[23]S. E. Kohn, P. Y. Yu, Y. Petroff, Y. R. Shen, Y. Tsang, and M. L. Cohen, Phys. Rev. B **8**, 1477 (1973).
[24]Y. Wang, A. Suna, W. Mahler, and R. Kasowski, J. Chem. Phys. **87**, 7315 (1987).
[25]P. E. Lippens and M. Lannoo, Phys. Rev. B **39**, 10 935 (1989).
[26]M. V. RamaKrishna and P. A. Friesner, Phys. Rev. Lett. **67**, 629 (1991); S. V. Nair, L. M. Ramaniah, and K. C. Rustagi, Phys. Rev. B **45**, 5969 (1992).
[27]Y. Wang and N. Herron, Phys. Rev. B **42**, 7253 (1990).
[28]G. T. Einevoll, Phys. Rev. B **45**, 3410 (1992).
[29]P. E. Lippens and M. Lannoo, Phys. Rev. B **41**, 6079 (1990).